REPORT DOCUMENTATION PAGE

Form Approved
OMB NO. 0704-0188

1. AGENCY USE ONLY (Leave Blank)	2. REPORT DATE	3. REPORT TYPE AND DATES COVERED
	31December 2009	Final report Oct 01, 2007 – Sep 30, 2009

4. TITLE AND SUBTITLE	5. FUNDING NUMBERS
Hearing Protection for High-Noise Environments	Contract No: FA9550-08-C-0006
6. AUTHOR(S) Elizabeth H. Bleszynski, Marek Ch. Bleszynski, Thomas Jaroszewicz, L. Demkowicz, P. Gatto, J. Kurtz, M. Paszynski, W. Rachowicz, M. Hamilton, and C. Champlin	
7. PERFORMING ORGANIZATION NAME(S) AND ADDRESS(ES) Monopole Research 739 Calle Sequoia Thousand Oaks, CA 91360	8. PERFORMING ORGANIZATION REPORT NUMBER MON-09-14L. Demkowicz
9. SPONSORING / MONITORING AGENCY NAME(S) AND ADDRESS(ES) Air Force Office of Scientific Research 875 N. Randolph Street, RM 3112 Arlington, VA 22203	10. SPONSORING / MONITORING AGENCY REPORT NUMBER not known

11. SUPPLEMENTARY NOTES
The views, opinions and/or findings contained in this report are those of the author(s) and should not be construed as an official Department of the Air Force position, policy or decision, unless so designated by other documentation.

12 a. DISTRIBUTION / AVAILABILITY STATEMENT	12 b. DISTRIBUTION CODE
Approved for public release, distribution is unlimited.	

13. ABSTRACT (Maximum 200 words)

The objective of our effort was

- to develop mathematical algorithms and high fidelity software tools which would allow identification and understanding of relevant bioacoustic and psychoacoustic mechanisms responsible for the transmission of acoustic energy through non-airborne pathways to the cochlea, and
- to apply these tools to significantly reduce the cost of subsequent experiments.

The integral-equation approach to solution of large elasto-acoustic problems, pursued in this project, offers valuable and unique advantages. The most important of these are:

- High accuracy characteristic of the integral-equation approach.
- Applicability to problems involving high-density objects immersed in air, with an exact treatment of the infinite background medium, and with special methods for accurate description of wave penetration through the high-contrast air-tissue interface.
- Applicability to large problems involving tens of millions of unknowns, and including fine, sub-millimeter scale, geometrical details.
- An efficient numerical implementation involving non-lossy compression of the stiffness matrix and distributed-memory parallelization.
- The developed code exhibits an approximately linear scaling of the computational cost with the number of unknowns, and almost perfect speedup with the number of processors.

When completed, the developed code should significantly broaden the scope and improve accuracy of realistic biomedical and safety-related application, of particular importance being analysis of effects of noise on human subjects, and assessment and design of noise protection devices. Such simulations are, at present, limited because of prohibitive memory and computational requirements as well as insufficient accuracy of currently available approaches.

-14. SUBJECT TERMS	15. NUMBER OF PAGES
Computational acoustics, integral equation formulation, fast compression techniques, Adaptive Integral Method, bone conducted sound, noise protection devices	1 + 14
	16. PRICE CODE not known

17. SECURITY CLASSIFICATION OR REPORT	18. SECURITY CLASSIFICATION ON THIS PAGE	19. SECURITY CLASSIFICATION OF ABSTRACT	20. LIMITATION OF ABSTRACT
UNCLASSIFIED	**UNCLASSIFIED**	**UNCLASSIFIED**	**UNCLASSIFIED**

Contract Title:

Hearing Protection for High-Noise Environments

Contract #: **FA9550-08-C-0006**

STTR Phase II – Final Report

Period of Performance: **Oct 01, 2007 – Sep 30, 2009**

Prepared by:

MONOPOLE RESEARCH
739 Calle Sequoia, Thousand Oaks, CA 91360
tel: (805) 375-0318 fax: (805) 499-9878

Contents

List of Figures

1 Description of the effort

The objective of our effort was

- to develop mathematical algorithms and high fidelity software tools which would allow identification and understanding of relevant bioacoustic and psychoacoustic mechanisms responsible for the transmission of acoustic energy through non-airborne pathways to the cochlea and,
- to apply these tools to significantly reduce the cost of subsequent experiments.

2 Main results

In the following subsections we summarize the main results of the development of mathematical algorithms and a high fidelity numerical solver to serve as a simulation tool for investigating such effects as, e.g., acoustic energy transfer to the inner ear via non-airborne pathways. The detailed description of the work performed is provided in the Attachments.

The solver is based on a modified form of the volumetric Lippmann-Schwinger integral equation, adapted to the treatment of high-contrast problems. It utilizes a stiffness matrix compression technique based on Fast Fourier Transform (FFT), and has been implemented on parallel distributed-memory systems. As a result, it allows simulations involving realistic geometries characterized by highly sub-wavelength details and large density contrasts, and described in terms of several million unknowns.

2.1 Development of integral-equation formulations and design of the solver for elasticity (Attachments 1 and 2)

Volumetric integral equations. We developed two formulations of volumetric integral equations in elasticity. The constructed versions are derived from the differential Lamé equation in either its first- or second-order form; this fact constitutes the rationale for considering two alternative types of equations: The first-order differential equations give rise to integral equations with more unknown functions and fewer (or lower order) derivatives of the functions themselves and the spatially dependent material parameters; whereas the more customary second-order equations result in integral equations for fewer unknown functions, but with higher-order derivatives.

Now, the presence or absence of gradients of material parameters in the equations is of critical importance in problems involving large-contrast discontinuities in the material properties, which, in our applications, always occur at the interface of the biological tissue with the surrounding air. We expect that, by using a formulation with fewer derivatives, we should be able to better control such gradient contributions in the equations. Nevertheless, both types of equations required extensive rearrangements, analogous to the reformulation of the conventional Lippmann-Schwinger (L-S) equations which we developed in the case of acoustics (Reference 2 in Section 6). By following analogous procedures in the present context of elasticity, we also arrived at the forms of equations allowing separation of the surface-type contributions of material discontinuities – a prerequisite for application of

the approach pursued in the above publication. The decision on which of the alternative formulations is better suited to our purposes will have to be based on further numerical experiments with the solver.

Surface integral equations. We also developed an integral-equation formulation (including the discretization procedure) of surface integral equations. Such a formulation is applicable to geometries composed of regions of piecewise homogeneous materials, and provides solutions for the displacement and traction fields $\mathbf{u}$ and $\mathbf{t}$, defined on interfaces separating different material regions. This type of formulation and its implementation plays several roles:

(a) It constitutes a very precise cross-verification tool for the developed volumetric integral-equation solver.

(b) It is more efficient than the volumetric formulation in modeling protective devices (e.g., such as helmets) of possibly complex geometries, but consisting of regions of homogeneous materials.

(c) It is useful in modeling fine details of the middle and inner human ear. These parts of the model include a number of intricately shaped volumetric regions filled with various homogeneous materials, and embedded in a larger volume of an inhomogeneous tissue. Those small regions can be then described in terms of displacement and traction fields defined only on their *surfaces*, thus eliminating the need of volumetric discretization, while inhomogeneous region is treated by means of a volumetric integral equation. We expect this approach to offer more flexibility and a better accuracy in modeling small complex geometries.

For a general problem involving a set of homogeneous regions Ω_m separated by interfaces, the obtained system of integral equations (derived by the direct method from the representation theorems for the displacement field) consists of two equations per interface S_{mn} separating the regions Ω_m and Ω_n. These equations represents contributions to the displacement field $\mathbf{u}$ on the interface S_{mn} due to the displacement and traction fields $\mathbf{u}$ and $\mathbf{t}$ on the same interface and on other interfaces, say S_{im}, forming boundaries of the regions Ω_m and Ω_m with other regions Ω_i, $i \neq m$, $i \neq n$.

The equations involve the Green functions for the displacement and traction fields in the considered material regions. In our formulation of the surface integral equations we are using a convenient form of the Green function $G(\mathbf{r})$ for the displacement field, explicitly incorporating cancellation of singularities of the Green functions $g_{\mathrm{C}}(r)$ and $g_{\mathrm{S}}(r)$ describing, respectively, propagation of compressional and shear waves. The above representation ensures that the tensorial component of the Green function is regular for $r \to 0$, while, without the cancellation, it would have contained a $\sim 1/r^3$ singularity. The reduced degree of singularity is particularly important in the discretization of the equations. Attachment 1 includes a discussion of this problem and contains explicit expressions for the relevant matrix elements.

Coupling of volume and surface solutions. In view of the application **(c)** mentioned in the previous paragraph, we also developed a novel formulation which allows coupling of the *surface* unknowns with the *volumetric* unknowns associated with the inhomogeneous medium.

An example of a system involving both volumetric and surface fields is visualized in Fig. 1: surface fields $\mathbf{u}$ and $\mathbf{t}$ are supported on the boundary $\partial\Omega_m$ of a homogeneous region Ω_m embedded in an inhomogeneous region Ω, supporting volumetric fields (here the displacement field $\mathbf{u}$). This configuration gives rise to three equations:
1. A volumetric equation in which the displacement $\mathbf{u}(\mathbf{r})$ at an observation point $\mathbf{r} \in \Omega$ is expressed in terms of the volumetric displacement $\mathbf{u}(\mathbf{r}')$ at a source point $\mathbf{r}' \in \Omega$ and in terms of the surface fields $\mathbf{u}(\mathbf{r}')$ and $\mathbf{t}(\mathbf{r}')$ at a source point $\mathbf{r}' \in \partial\Omega_m$.
2. A set of two surface equations for the fields $\mathbf{u}(\mathbf{r})$ and $\mathbf{t}(\mathbf{r})$ at $\mathbf{r} \in \partial\Omega_m$, also expressed in terms of the volumetric field $\mathbf{u}(\mathbf{r}')$ and surface fields $\mathbf{u}(\mathbf{r}')$ and $\mathbf{t}(\mathbf{r}')$.

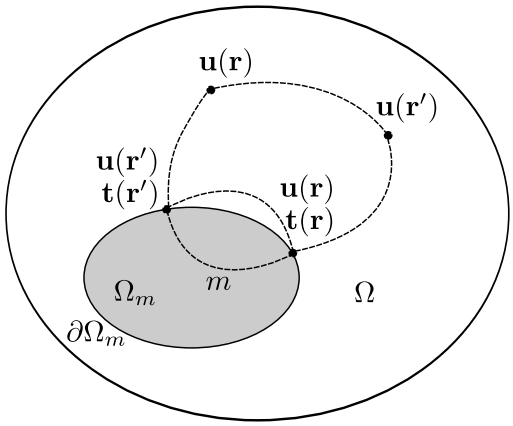

Figure 1: A schematic representation of a system of coupled integral equations for volumetric and surface displacement and traction fields. The broken lines without an index and with the index m represent, respectively, the Green functions in the background medium and in the homogeneous region Ω_m.

Analytical formulation for computation of matrix elements. We derived explicit expressions for the many types of Galerkin matrix elements arising in the developed formulations of surface and volumetric elasto-acoustic integral equations. These formulations involve scalar, vectorial, and tensorial unknowns, as well as first and second derivatives of the Green functions. As a result of application of integral identities involving integration by parts, we were, generally, able to reduce the dimensionalities of the integrals and reduce the degree of their singularities. The details are contained in Attachment 2.

Implementation. We designed the general structure of the solver code for elasticity (which also includes acoustics, as a special case). It comprises an extensible library of relatively simple routines for constructing particular blocks and sets of matrix elements, as well as their compressed representations, appearing in various integral-equation formulations.

These routines create input data used by a general routine whose task is to assemble the entire matrix and store it in a compressed form.

We have implemented a part of this scheme, corresponding to acoustic volumetric equations in first- and second-order formulations.

2.2 Construction of analytic solutions for a layered elastic sphere (Attachment 3)

We constructed a program evaluating the analytic series solution for a layered elastic sphere. It provides a complete distribution of the displacement and other related fields inside a multi-layer sphere consisting of an arbitrary number of layers, each characterized by any desired value of density ρ and the Lamé parameters λ and μ. The sphere is embedded in an infinite acoustic medium (e.g., air) and subject to an acoustic plane wave propagating in that medium.

We have used the series solution code to check the accuracy of our volumetric integral equation solver in a number of representative cases, including layers of materials encountered in modeling of a human head and a helmet, such as steel, cork, skin, fat, muscle, brain tissue and bone.

The code has also played a very instrumental role in the verification of the Finite Element Method solver for elasticity developed by the University of Texas team members.

2.3 Parallelization of the integral-equation solver (Attachment 4)

We significantly improved the previous version of our distributed-memory acoustic solver. The main modifications were related to the FFT matrix compression scheme, and their purpose was to reduce the memory requirements of the code. This goal was achieved by improving the structure of the data layout and the order of operations, without any deterioration of the compression accuracy. The two main implemented improvements, described in more detail in the Attachment, were:
(i) Reorganizing the procedure of computation of coefficients (denoted by V) mapping the physical pressure sources to equivalent sources defined on a Cartesian grid (and subsequently used by Fast Fourier Transforms). Most of these coefficients are now computed on-the-fly, and do not require any storage.
(ii) Storing the V coefficients as a sparse matrix, in which each processor computes and saves only the coefficients associated with the Cartesian grid nodes owned by that processor.
The first of these changes eliminated a temporary increase of the storage during matrix construction. The second reduced the size of the compressed stiffness matrix in its final form. The overall effect of these improvements depends on the number of Cartesian grid nodes per processor, and is most significant when the Cartesian grid covering the object is partitioned into thin "slices" assigned to the processors. For such problems as reported in the Attachment 4, the maximum memory per processor decreased, due to changes in the code, by at least 30 % and, in many cases, by significantly more. This reduction eliminated the need of requesting more storage than the default amount (1.75 GB per processor) and thus significantly facilitated the computations.

We also developed and implemented in the solver an enhanced version of our two-stage algorithm for problems involving large density contrasts. The modified version uses an alternative discretization procedure in the first solution step (i.e., in the surface problem). It was found to accelerate convergence and increase the size of tractable geometrically complex large-contrast problems up to eight million unknowns.

2.4 Construction of head geometry with a detailed ear structure (Attachment 5)

Geometry of the middle and inner ear constitutes a highly intricate structure. We realize that precise modeling of those elements is essential for reliable numerical simulation which could discern between different mechanisms of energy transfer to the human ear.

Therefore, apart from attempting to construct an efficient mathematical formulation, a significant fraction of our effort was devoted to the construction of a sufficiently detailed and anatomically faithful model of the ear (its outer, middle, and inner parts).

We have built a rather detailed model, including what we thought were the essential geometry elements in simulating energy transfer processes. The geometry consists of:

1. the outer ear represented by its exterior surface, the surface of the auditory canal, and including the tympanic membrane, modeled as a finite-thickness surface;
2. the middle ear, consisting of the system of ossicles and supporting structures;
3. the skull, described by the surface of the bone, and including
4. the inner ear, modeled as a set of surfaces representing the boundaries of the cochlea, the vestibule, and the semi-circular canals; and
5. the outer surface of the skin surrounding the skull.

For tests of noise-protection devices, we also constructed a model of a helmet and the material layer filling the space between the helmet and the surface of the head.

We stress that all the geometry components: skull, skin, inner, middle, and outer ear, as well as the helmet, are mutually compatible and matched to one another. This fact is illustrated by the example in Fig. 2, which shows the outer and inner ear together with a part of the skull. Other representative examples of the geometry details are presented in Attachment 5.

We note that our work on the geometry construction is not fully completed. We continue our work in this area and should be in a position to start computations employing this detailed model within two to three months.

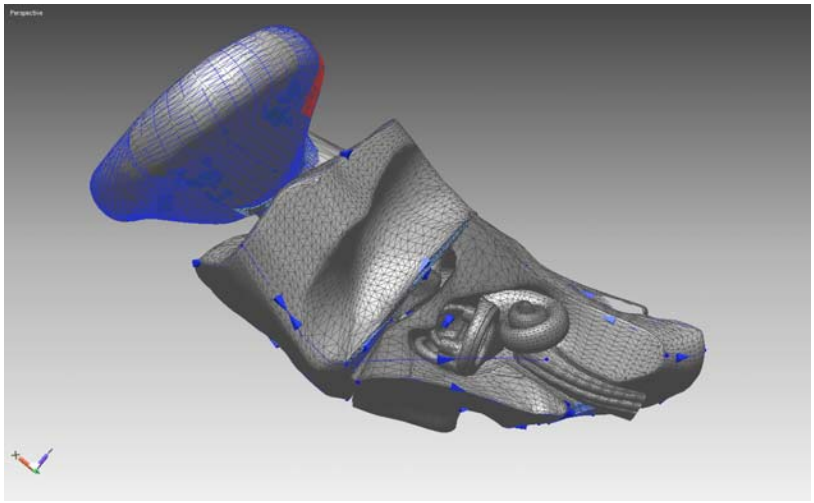

Figure 2: The outer ear and the inner ear structure embedded in the skull bone.

2.5 Numerical simulations (Attachment 4)

We carried out an extensive set of numerical simulations of pressure distribution in the human head models, including also models of helmets. We used both realistically shaped models of the head and helmets, as well as simplified geometries (such as layered spheres and spherical shells) to perform code verification against the analytical series solutions.

The problems involved up to about 10 million unknowns, and were solved on up to 200 processors.

In particular, our solver has been applied to a number of representative problems involving a model of a human head enclosed in a helmet, with the in-between space filled with an elastic material. The head and helmet geometries were also used in thorough tests of the accuracy of the matrix compression used in the solver; the tests, described in Attachment 4, involved comparison of solutions obtained with various geometry discretizations and compression parameters.

Some results of these simulations were reported in a paper presented at the 2009 MEMRO conference at Stanford University (Attachment 7) and accepted for publication in Hearing Research.

As one of the tests, we compared pressure distributions in the head model, computed with a coarser ($N \simeq 400,000$ unknowns) and a finer ($N \simeq 2,700,000$) discretization. The results, shown in Fig. 3, demonstrate a good agreement between the results obtained in these two cases.

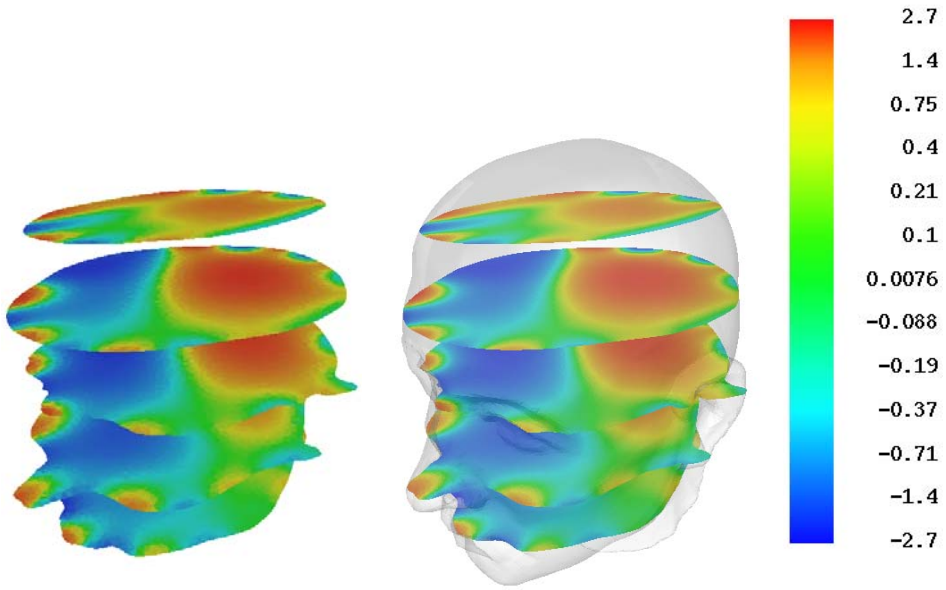

(a) (b)

Figure 3: Distributions of the real part of the pressure, plotted in the logarithmic scale, on several sections in the axial plane of the human head model with (a) a coarser discretization ($N \simeq 400,000$ tetrahedra), and (b) a finer discretization ($N \simeq 2,700,000$ tetrahedra). The models are subject to an acoustic wave of unit pressure amplitude and frequency 5 kHz, incident horizontally on the right ear. In (b) the outline of the head outer surface is superimposed on the pressure distributions.

As another example, we compared pressure distributions in the isolated head model and in the same model with an addition of a steel helmet separated from the head by a layer of cork. The geometry of the head and the helmet is shown in Fig. 4; the surface of the head belongs, actually, to the set of the matching geometry elements described in Sec. 2.4 above and in Attachment 5.

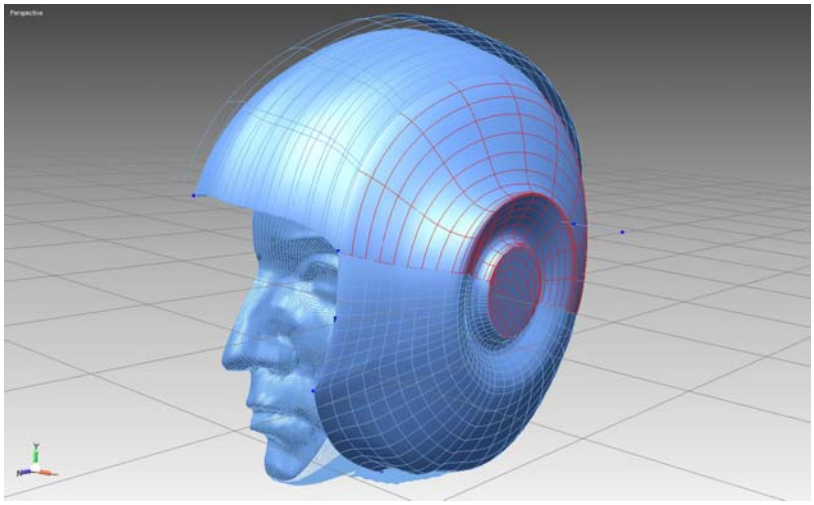

Figure 4: The matched models of the head skin surface and the helmet.

The head and head+cork+helmet geometries were discretized, respectively, with $N \simeq 2,700,000$ and $N \simeq 4,700,000$ tetrahedra, and the solutions were computed on 108 and 128 processors. The results of the computations are visualized, as distributions of the absolute value of the pressure in the coronal plane of the models, in Fig. 5. The solutions show a nontrivial behavior and exhibit physical phenomena which may be relevant in the design of protective devices:

- In the first case (Fig. 5(i)) the pressure is maximal at the entrance to the ear canal, and it is smoothly distributed inside the head. The solution for the pressure is, actually, suggestive of a resonance-type (P-wave) behavior, as the pressure changes sign along the approximately vertical line seen in the Figure.

- The solution for the head and helmet system (Fig. 5(ii)) is very different. It exhibits a distinct oscillatory behavior along the surface of the helmet and in the region filled by cork. This region appears to have properties of a "waveguide": because of the cork density being significantly lower than that of the surrounding materials (the helmet and the head), and the resulting impedance mismatch at the boundaries, the wave tends to be trapped in that area.

We also note that, although the presence of the helmet with a cork lining completely changes the pressure distribution inside the head, it does not reduce its maximum value (the data Figs. 5(i) and 5(ii) are rendered in different scales). It can be expected, however, that the physical picture of wave propagation should strongly depend on the properties of the layer filling the head-helmet gap, and could be quite different for a dissipative and strongly damping (e.g., porous) material.

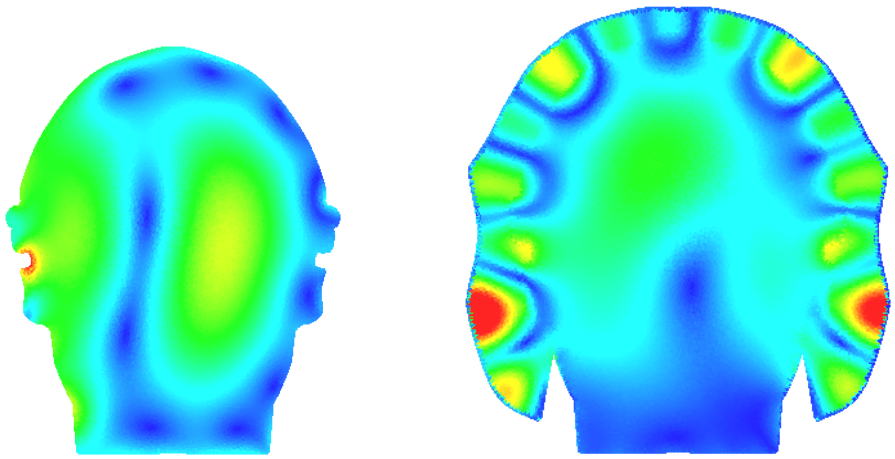

(i) (ii)

Figure 5: Pressure distributions in the coronal plane for (i) the human head model and (ii) the system consisting of the human head and a steel helmet models, with the in-between space filled by cork. The numbers of unknowns in these two problems are $N \simeq 2,700,00$ and $N \simeq 4,700,00$. The maximum pressure values are about 4 in (i) and 15 in (ii).

2.6 The University of Texas team contribution – Finite Element analysis (Attachment 6)

The University of Texas team contribution focused on the Finite Element Method (FEM) solver for elasticity.

Members of the team have enhanced their Finite Element Code to include simultaneously tetrahedral, hexahedral, pyramidal, and prism elements. They also developed a schematic geometrical model of the middle ear, which is, however, expected to capture essential physical mechanisms of energy transfer. This model has been used in simulations with the Finite Element code. The details of these developments are described in the Attachment.

3 Benefits and technical feasibility of the developed approach

The integral-equation approach to solution of large elasto-acoustic problems, pursued in this project, offers valuable and unique advantages. The most important of these are:

- High accuracy characteristic of the integral-equation approach.
- Applicability to problems involving high-density objects immersed in air, with an exact treatment of the infinite background medium, and with special methods for accurate description of wave penetration through the high-contrast air-tissue interface.
- Applicability to large problems involving tens of millions of unknowns, and including fine, sub-millimeter scale, geometrical details.

- An efficient numerical implementation involving non-lossy compression of the stiffness matrix and distributed-memory parallelization. The developed code exhibits an approximately linear scaling of the computational cost with the number of unknowns, and almost perfect speedup with the number of processors.

When completed, the developed code should significantly broaden the scope and improve accuracy of realistic biomedical and safety-related application, of particular importance being analysis of effects of noise on human subjects, and assessment and design of noise protection devices. Such simulations are, at present, limited because of prohibitive memory and computational requirements as well as insufficient accuracy of currently available approaches.

4 List of attachments

Detailed technical descriptions of the developments summarized in Section 2 are contained in the Attachments listed below.

- Attachment 1 gives extensive details of the integral-equation formulations developed in this effort, including several forms of surface and volume integral equations, treatment of high-contrast problems, and explicit formulae for the resulting matrix elements. It also describes the general design of the solver code.

- Attachment 2 presents details of a representation of the matrix elements appearing in our integral-equation formulations, well suited (through reductions in integral dimensionalities and degrees of their singularities) for numerical computation.

- Attachment 3 includes the formulation and implementation of the exact series solution for multi-layer sphere characterized by arbitrary elastic properties of the layers, subject to a plane-wave incident acoustic field.

- Attachment 4 describes the implemented parallel version of our acoustic solver, and includes illustrative examples of large-scale computations, serving also as tests of the accuracy of the solutions. The implementation described there includes improvements (relative to the previous code version), allowing a significant reduction in the required storage. Part of the material in this Attachment constitutes a paper being prepared for publication.

- Attachment 5 includes representative examples of details of the constructed inner ear geometry.

- Attachment 6 contains contribution of the University of Texas at Austin team.

- Attachment 7 contains the paper presented at the MEMRO 2009 conference and accepted for publication in Hearing Research.

5 Articles and conference contributions resulting from current project

1. Elizabeth Bleszynski, Marek Bleszynski, and Thomas Jaroszewicz, "A fast FFT-based integral equation solver for simulation of elastoacoustic wave propagation in human head," J. Acoust. Soc. Am., Vol. 123, No. 5, p. 3565 (Acoustics'08 Paris).

2. Elizabeth Bleszynski, Marek Bleszynski, and Thomas Jaroszewicz, "Numerical simulation of propagation of acoustic and elastic waves in human head with fast integral equation solver," J. Acoust. Soc. Am., Vol. 125, No. 4, p. 2650.

3. Elizabeth H. Bleszynski, Marek K. Bleszynski, and Thomas Jaroszewicz, "Acousto-elastic integral equation based numerical simulation tools for analysis of sound wave interactions with human head hearing system and design of high-noise protection devices," Hearing Research (in press).

6 Related articles published during reporting period

1. E. Bleszynski, M. Bleszynski, and T. Jaroszewicz, "Fast volumetric integral-equation solver for acoustic wave propagation through inhomogeneous media," J. Acoust. Soc. Am., Vol. 124, No. 1, pp. 396–408.

2. E. Bleszynski, M. Bleszynski, and T. Jaroszewicz, "Fast volumetric integral-equation solver for high-contrast acoustics," J. Acoust. Soc. Am., Vol. 124, No. 6, pp. 3684–3693.